JOURNAL OF GEOPHYSICAL RESEARCH, VOL. 106, NO. D4, PAGES 3371–3380, FEBRUARY 27, 2001

Adjusting for sampling density in grid box land and ocean surface temperature time series

P. D. Jones, T. J. Osborn, and K. R. Briffa
Climatic Research Unit, University of East Anglia, Norwich, U K.

C. K. Folland, E. B. Horton, L. V. Alexander, D. E. Parker, and N. A. Rayner
Hadley Centre for Climate Prediction and Research, The Meteorological Office, Bracknell, Berkshire, U.K.

Abstract. We develop methods for adjusting grid box average temperature time series for the effects on variance of changing numbers of contributing data. Owing to the different sampling characteristics of the data, we use different techniques over land and ocean. The result is to damp average temperature anomalies over a grid box by an amount inversely related to the number of contributing stations or observations. Variance corrections influence all grid box time series but have their greatest effects over data sparse oceanic regions. After adjustment, the grid box land and ocean surface temperature data sets are unaffected by artificial variance changes which might affect, in particular, the results of analyses of the incidence of extreme values. We combine the adjusted land surface air temperature and sea surface temperature data sets and apply a limited spatial interpolation. The effects of our procedures on hemispheric and global temperature anomaly series are small.

1. Introduction

The irregular geographical distribution of land and ocean surface temperature measurements must be accounted for when making estimates of regional, hemispheric, and global average temperature departures (anomalies) from climatology. This is generally accomplished by interpolating the basic data, in the form of anomalies, to a regular set of grid points [e.g., *Jones et al.*, 1986] or by averaging the data, possibly with weighting, into boxes, which may be of equal area [e.g., *Hansen and Lebedeff*, 1987; *Bottomley et al.*, 1990; *Jones*, 1994; *Parker et al.*, 1995; *Peterson et al.*, 1998; *Hansen et al.*, 1999]. Whichever method is used, the accuracy of the interpolated grid point or grid box value will depend on the density of available data. A high density will result in more accurately estimated values.

Data density has changed substantially over the last 150 years, affecting the variance of grid box values and hence the time series of larger-scale values. The sparser database for early years over both land and marine areas yields a more variable series than does recent denser coverage. Furthermore, nearby grid box series may have different variances over any particular epoch merely because one series is based on more observations than another (see *Osborn and Hulme* [1997], for an example based on precipitation). Heterogeneous variance in space and time affects estimates of correlation matrices and, particularly, covariance matrices, which are used in principal component analysis/empirical orthogonal function (PCA/EOF) techniques. Homogenization of the variance benefits such analyses and is particularly important for making consistent assessments of the occurrence of extreme monthly, seasonal, or annual temperatures [*Jones et al.*, 1999a] and of temporal changes in temperature variability. The method developed below for land-based data can also be easily adapted to related sciences (e.g., hydrology) where the computation of areal rainfall estimates can be corrected for the numbers of gauges being used [see *Wigley et al.*, 1984; *Osborn and Hulme*, 1997].

The purpose of this paper is to develop monthly gridded data sets of both land surface air temperature and sea surface temperature (SST) that contain as far as possible no artificial variations in variance due to changing amounts of data. Over land we extend the *Jones et al.* [1997] methods (originally devised to assess the standard error of hemispheric and global temperature estimates) to adjust the grid box temperature series for changes in the number of contributing stations through time and to reduce all series to a consistent level of variance. Over the oceans the variations in data density in given regions are caused by a rapidly changing distribution of observations, so we use a different method which builds on the quality control and gridding procedures for SST developed by *Bottomley et al.* [1990] and *Parker et al.* [1995]. After variance correction the land and marine components are recombined into a single data set (HadCRUTv) using the methodology given by *Jones et al.* [1999b]. Combination of the two fields is discussed in more detail than previously.

Paper number 2000JD900564.
0148-0227/01/2000JD900564$09.00

2. Theory of Adjustments

2.1. Land

The basic formula used by *Jones et al.* [1997], which has been used in various guises, particularly in hydrology and dendroclimatology [e.g., *Yevjevich*, 1972; *Wigley et al.*, 1984; *Briffa and Jones*, 1990; *Parker et al.*, 1992; *Kagan*, 1997; *Briffa et al.*, 1998], relates the variance of the area average to the station variance

$$S_n^2 = \overline{s_i^2}\,(1 + (n\text{-}1)\bar{r})/n, \quad (1)$$

where S_n^2 is the variance of the grid box (area average) time series, $\overline{s_i^2}$ is the average variance of the site time series within the grid box, and $\bar{r}$ is the average inter site correlation of the n available sites. Equation (1) assumes that the values of $\overline{s_i^2}$ do not vary greatly within a grid box, an assumption that should be easily satisfied for the small grid boxes used here. The subscript n in S_n^2 indicates the number of sites involved. *Parker et al.* [1992] and *Osborn et al.* [1997] showed that sampling at every point and letting $n \to \infty$, (1) is reduced to

$$S_\infty^2 = \overline{s_i^2}\,\bar{r}\ . \quad (2)$$

Because of interdependence between the n stations within each grid box, there are less than n independent samples. It can be shown [e.g., *Yevjevich*, 1972] that the number of effectively independent samples (n_{eff}) is

$$n_{\text{eff}} = n/(1 + (n\text{-}1)\bar{r}). \quad (3)$$

If here $n \to \infty$ the maximum value n_{eff} can take n_∞ is

$$n_\infty = 1/\bar{r}\ . \quad (4)$$

Thus to estimate S_∞^2 through time, allowing for changing n, and reducing the value to a consistent level, we combine these four equations to yield

$$S_\infty^2 = S_n^2\, n_{\text{eff}}/n_\infty \quad (5)$$

To apply (5) to any time series the series is expressed in the form of anomalies and multiplied by $(n_{\text{eff}}/n_\infty)^{1/2}$ [see *Osborn et al.*, 1997, equation 7]. This both reduces the variance and makes it more consistent in time by compensating for the changes of n_{eff}. In addition, the difference in variance between grid boxes is reduced as account is automatically taken of the differences of n_{eff} and n_∞ between grid boxes. A restriction is that the theory requires a stationary time series. Real long-term temperature changes, which for some grid boxes have been up to 2°C over the last 130 years, would have biased the adjustments if we had used a fixed base for anomalies, such as 1961-1990. Adjustments would have been greater for periods much warmer or cooler than 1961-1990, compared to periods with temperatures nearer to the 1961-1990 average. We therefore created smoothed time-varying base series using a Gaussian-weighted filter that passes variations on timescales exceeding about 30 years. We then applied the adjustments to the high-frequency residuals from these series. Our implicit 30-year high-pass filter produces a stationary series but retains interdecadal variability. Tests on some grid boxes using residuals from a 10- or 50-year filter showed only minor differences in the final adjusted data. Ambiguities in the choice of high-pass filter therefore are not important compared to the need for the efficient removal of the long-term trend.

Note that this method copes with problems due to data gaps but does not consider the random instrumental error as is done below for the marine data. We do not regard this as a significant problem because the random instrumental errors are substantially less than for marine data, and the variance of the land temperature signal is often larger. Monthly land station averages are based on daily station averages so at least 60 observations per month are made for each station.

2.2. Ocean

For the oceans we estimate the contribution of data noise over a grid box from an underlying set of data that are mainly from moving ships and therefore come from any part of the grid box. The fundamental problem to be solved involves distinguishing the noise due to the gaps in data, and the inherent observational uncertainties, from the true signal. The signal is estimated as an anomaly from a long-term climatology and is assumed to consist of a large-scale and a local component. The noise is assumed to be a random deviation from the sum of the climatology and the estimated signal. The variance of the noise in a monthly mean anomaly is assumed to depend inversely on the number of quality-controlled ship observations in the grid box.

We assume that an estimate of the large-scale component of the signal can be obtained from global- and ocean-basin-scale eigenvector reconstructions of SST anomaly fields. This could employ the eigenvector projection method [*Rayner et al.*, 1996], but here we use the somewhat better method of reduced space optimum interpolation [*Kaplan et al.*, 1998]. This is little influenced by the local noise itself in data-sparse regions. To achieve this, we use the reconstructions that form a key stage in the production of the new Hadley Centre sea ice and sea surface temperature (HadISST1) data set (N.A. Rayner et al., HadISST1: Global sea ice and sea surface temperature, 1871-1999, manuscript in preparation, 2000) (hereinafter referred to as Rayner et al., manuscript in preparation, 2000).

We now assume that the true additional local-scale signal in grid-box i, superimposed on the eigenvector-based estimate of the large-scale signal, is Δt_{ti}, the observed deviation is Δt_i and the random observational error is ε_i. The random observational error includes instrumental errors and sampling errors that are due to real small-scale SST features that cannot be resolved by the grid box average. We also assume that $\overline{\varepsilon_i} = 0$ is the expected value of the random error. Then

$$\Delta t_i = \Delta t_{ti} + \varepsilon_i \quad (6)$$

Because true deviations are uncorrelated with the errors,

$$\overline{\Delta t_i^2} = \overline{\Delta t_{ti}^2} + \overline{\varepsilon_i^2}\ . \quad (7)$$

Thus the variance of deviations about the background signal is inflated by random errors.

To correct this, we multiply each value of Δt_i by a factor k where $0 < k < 1$. We require

$$k^2\overline{\Delta t_i^2} = \overline{\Delta t_{ti}^2} \text{ so that } k=1 \text{ when } \Delta t_i = \Delta t_{ti}.$$

From (7) we easily find that

$$k = \sqrt{\frac{\overline{\Delta t_i^2} - \overline{\varepsilon_i^2}}{\overline{\Delta t_i^2}}}\ , \quad (8)$$

where $\overline{\varepsilon_i^2}$ is based on separately estimated statistics of the random observational error and sampling error from individual observations. For an individual observation we let these combined errors (the form normally available) be ε'_i. Then assuming the errors of the n individual observations in the grid are spatially uncorrelated,

$$\overline{\varepsilon_i^2} = \frac{\overline{\varepsilon'^2_i}}{n}\ . \quad (9)$$

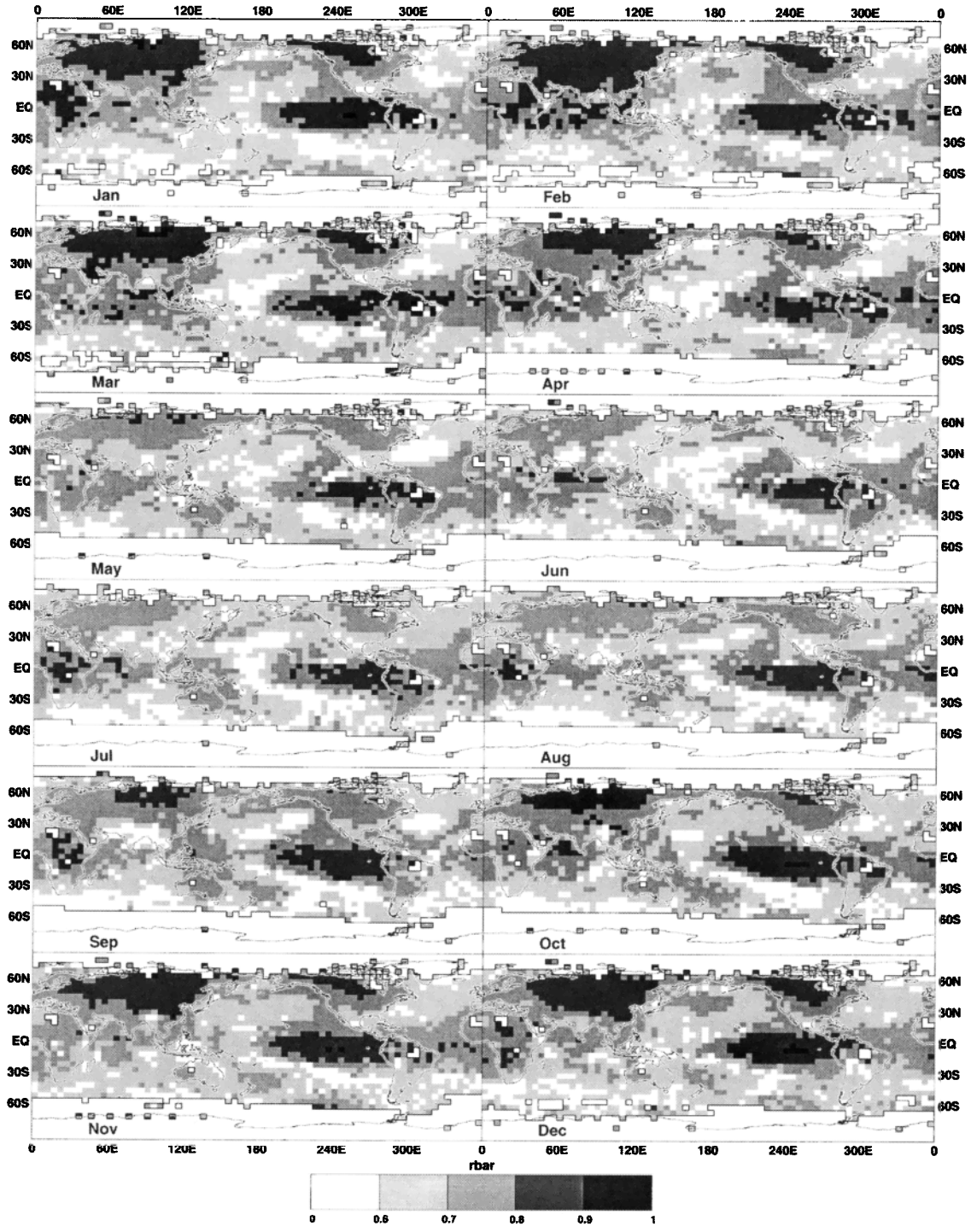

Figure 1. Monthly values of high-frequency $\bar{r}$, calculated using residual (from the low-pass (> 30 years) Gaussian-weighted filter) grid box temperatures from the *Jones et al.* [1999b] data set of combined land and sea surface temperature data. The blank outlines surround those boxes with less than 20 years of data available for computing correlations.

The marine data were available in two forms. Most of the data were trimmed 5-day 1° latitude x 1° longitude area mean anomalies based on the Meteorological Office Marine Data Bank (MDB [Bottomley *et al.*, 1990]). We supplemented these with monthly 1° latitude x 1° longitude area median anomalies interpolated from the 2° resolution Comprehensive Ocean-Atmosphere Data Set (COADS [*Woodruff et al.*, 1987]) up to 1959 and thereafter taken directly from the 1° resolution COADS-Pan-American Climate Studies data set [*Woodruff et al.*, 1998] which was derived using 4.5σ trimming limits. In each case, we expressed the anomalies as residuals relative to the sum of the climatology and the background signal. Tests showed that the mean correlations between the MDB residuals within individual months and 5° latitude by 5° longitude grid boxes were close to zero in over 95% of grid boxes. So we were able to use the above theory without resorting to more complex procedures such as optimum averaging [*Kagan*, 1997] of residuals.

The different statistical character of the MDB and our form of the COADS data required some changes in the details of the adjustment procedures. First, the same estimates of ε_i' for individual observations were used for each type of data. Estimates of measurement error variance β^2 taken from *Kent et al.* [1999] were added to estimates of sampling error variance α^2 derived from the variance of MDB-based 5-day 1° x 1° area mean anomalies within monthly 5° x 5° area samples. The result was multiplied by 0.75 to give $\varepsilon_i'^2$ because α^2 and β^2 are both likely to include common contributions, each assumed arbitrarily but plausibly to be about one third, from measurement and sampling error respectively. However, we used different expected variances $\overline{\Delta t_i^2}$ for the MDB and COADS data, calculated separately from MDB and COADS residuals from the sum of the climatology and the background signal. The COADS residuals, after multiplying by k and adding back to the first guess, were only used in 5° area grid boxes in HadISST1 where no MDB data were available.

The coverage of marine data is slightly reduced compared to *Parker et al.* [1995] because we applied additional quality controls to the 5-day mean 1° x 1° area anomalies. From these anomalies we first calculated 1956-1995 climatological averages μ_c and standard deviations σ_c for each 1° x 1° area for each 5-day calendar interval. For the same period we also calculated climatological standard deviations σ_d of the differences between the 5-day mean 1° x 1° area anomalies and the simultaneous average anomaly in the eight neighboring 1° x 1° areas. In the subsequent quality control, an anomaly without neighbors was rejected if it differed from μ_c by more than $1.64\sigma_c$. In addition, an anomaly with only one neighbour was rejected if its difference from μ_c exceeded $1.64\sigma_c$, and it differed from its neighbor by

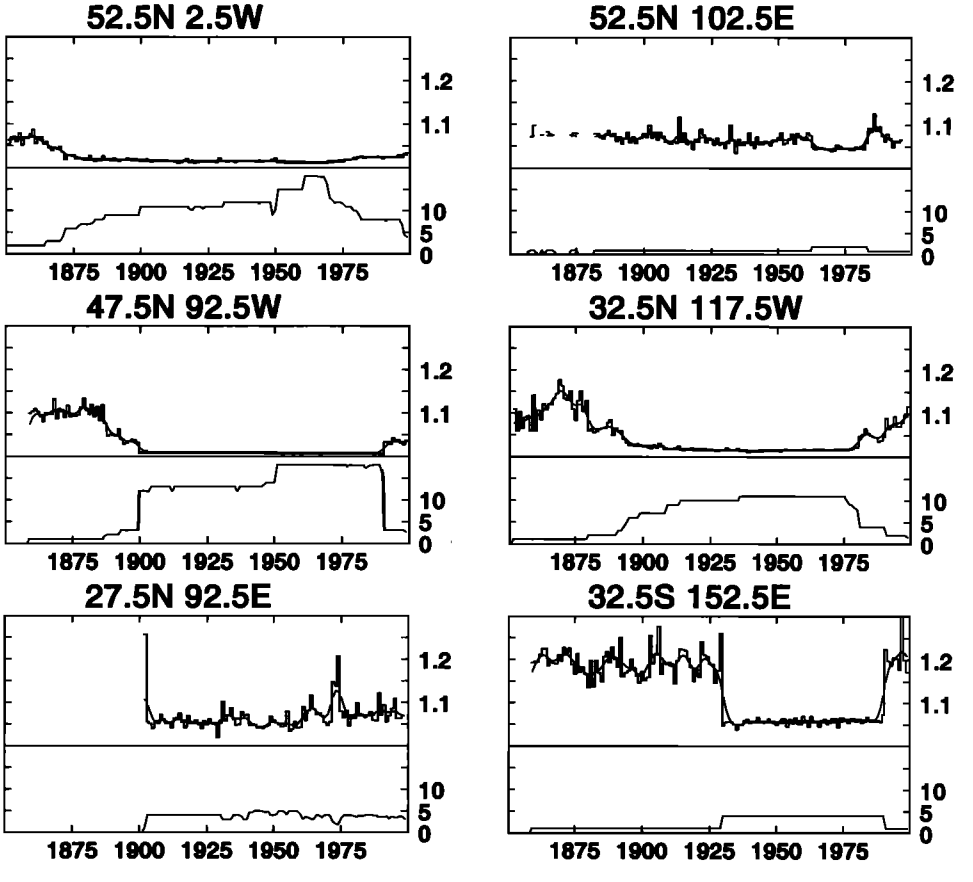

Figure 2. Statistics of monthly land grid box air temperature anomaly (°C) time series before and after correction. The top plot of each plot shows the ratio of the standard deviations of the 12 months for each year (before/after). The series of ratios is also shown smoothed with a 10-year Gaussian filter. The bottom part of each plot shows the number of contributing stations through time at that grid box. The grid boxes, on a 5° latitude by 5° longitude basis, are given with respect to their central location.

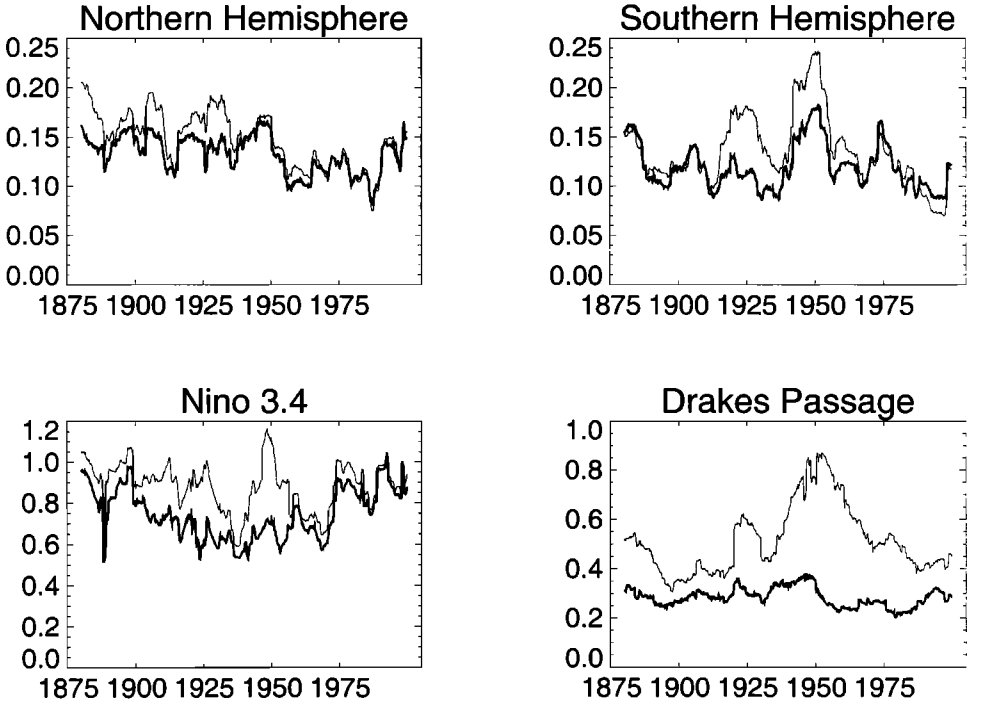

Figure 4. Ten-year running-mean standard deviations (°C) over 120 months of original (thin) and adjusted (thick) monthly SST anomalies for the same regions as shown in Figure 3.

more than $1.64\sigma_d$. Anomalies with two or more neighbors were accepted if they differed from the average of their neighbors by no more than $1.64\sigma_d$ and replaced by this average otherwise. Individual observations had already been through one level of quality control, and the rather strict criteria when comparing against the 1956-1995 climatology in this second quality control resulted in a loss of less than 5% of 1° x 1° area anomalies in each 5-day period. The incidence of local "bull's eyes" in monthly anomaly fields in relatively data-sparse regions was significantly reduced.

3. Application and Discussion

3.1. Land

We use the *Jones* [1994] grid box temperature anomaly series where station temperature data, expressed as anomalies from the 1961-1990 base period, are averaged within each grid box. We calculate $\bar{r}$ using the method given by *Jones et al.* [1997] using correlation decay lengths between grid box averages (their equation (9)); *Jones et al.* [1997] give reasons why the computation of $\bar{r}$ using the station data themselves is problematical. Separate fields of $\bar{r}$ are produced for each month, using the residuals from a low-pass (>30 years) Gaussian-weighted filter fitted through each monthly grid box time series. Using this approach enables stationary, detrended $\bar{r}$ values to be estimated for all grid boxes with data, even those where $n \leq 2$. To improve the estimates of $\bar{r}$ for coasts and islands, we calculated the correlation decay lengths using the combined (filtered) land and marine 5° x 5° grid box data set [*Jones et al.*, 1999b]. This enables better estimates of $\bar{r}$ to be made. Estimation of $\bar{r}$ from land data alone would have proved impossible for coastal and island grid boxes which sometimes have very few neighbors in the original land-only form. Because the $\bar{r}$ fields cover oceanic areas, they are near global.

Figure 1 shows spatial patterns of detrended values of $\bar{r}$ by calendar month. Values are highest (>0.9) over continental interiors, particularly in winter, and over some tropical ocean areas, especially the eastern equatorial Pacific throughout the year and the tropical Indian Ocean in some seasons. Lower $\bar{r}$ values (<0.7) occur in summer and over many other oceanic regions (midlatitude Southern Ocean, much of the North Pacific and North Atlantic). The spatial patterns of detrended $\bar{r}$ are qualitatively very similar to those of interannual variance $\overline{s_i^2}$ [see, e.g., *Jones et al.*, 1997]. Including the low-frequency component in $\bar{r}$ calculations raises $\bar{r}$ values as expected, particularly over mid- to high-latitude oceanic areas (as evident in the work by *Jones et al.* [1997, Figure 6]. These higher $\bar{r}$ values are, however, not strictly applicable in this paper.

We now apply (5) to the residuals of the 30-year Gaussian filter and then add back the filtered series. Figure 2 shows the ratio of the standard deviation of the 12 monthly temperature anomalies for each year before and after the application of (5) for six grid boxes. The panels are chosen to have contrasting variations in n through time and to cover a range of monthly $\bar{r}$ values from 0.6 to 0.9. Reductions in variance are strongly related to n. The ratios in Figure 2 fluctuate from year to year due to climate variability as corrections to the standard deviation will be greater for years when larger magnitude anomalies occur in months with smaller $n_{\text{eff}}/n_{\infty}$, that is, smaller values of $\bar{r}$. For individual grid boxes on the annual timescale, differences in anomalies before and after adjustment are only in the range ±0.20°C. Differences on a monthly timescale may be as large as ±0.50°C, but the effects partly cancel for annual values as monthly anomalies of different sign usually occur during the year. Note that a reduction in standard deviation will always

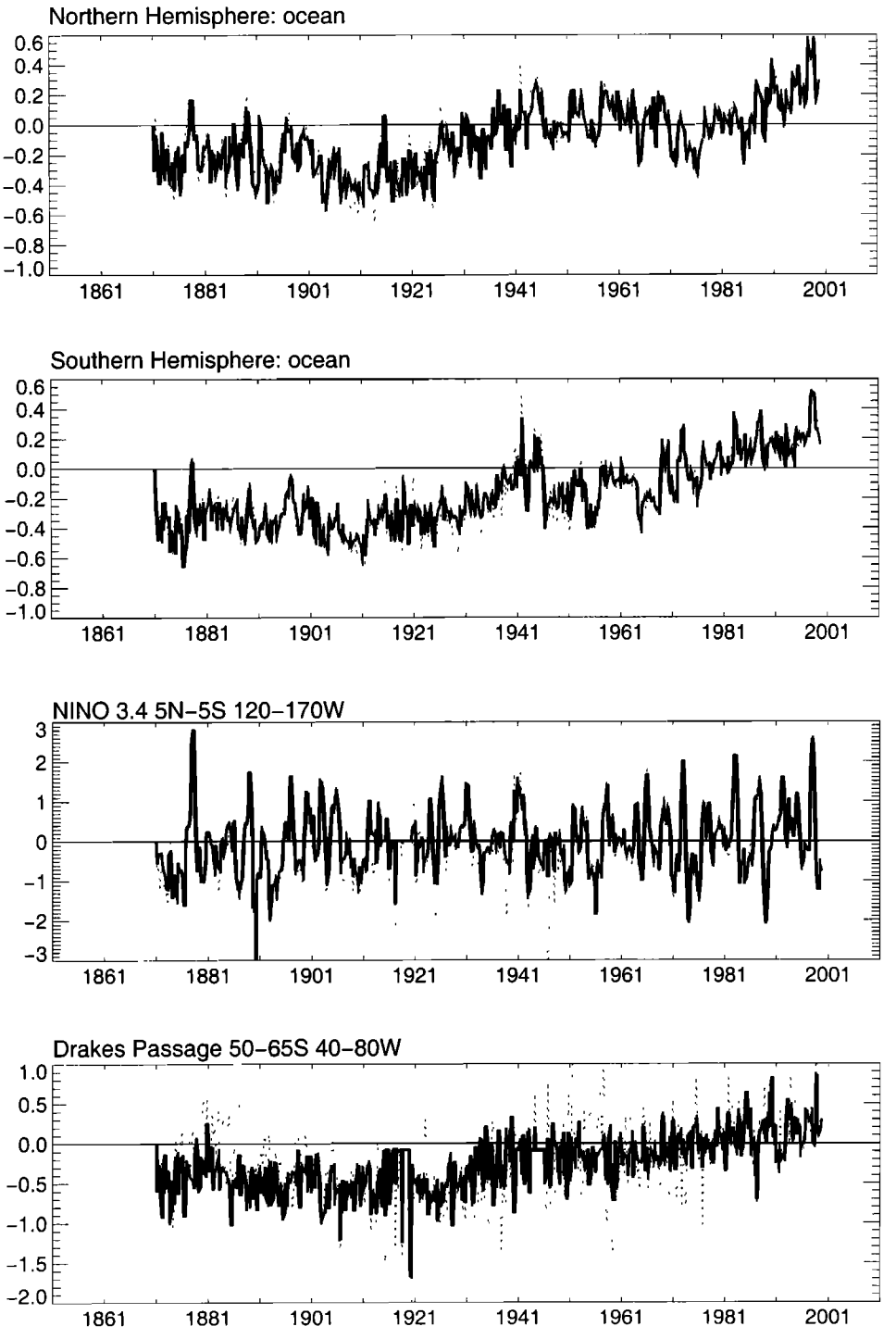

Figure 3. Original (dotted) and adjusted (solid) series of seasonal (January to March, etc.) SST anomalies (°C), relative to the 1961-1990 climatology, for the Northern Hemisphere, Southern Hemisphere, the Niño 3.4 area (5°N-5°S, 120°-170°W), and the Drake's Passage area (50°-65°S, 40°-80°W).

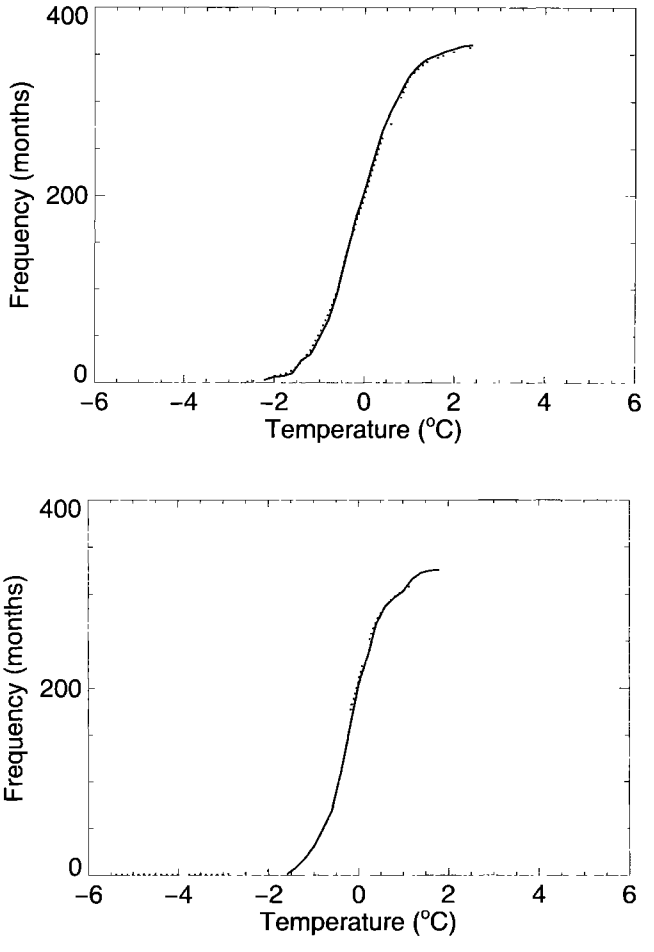

Figure 5a. Cumulative frequency distributions for average monthly temperature anomalies over the Niño3.4 area for adjusted (solid) and unadjusted (dotted) data over (top) 1961-1990 and (bottom) 1921-1950. The anomalies are with respect to 1961-1990 throughout.

occur due to this procedure, so the standard deviation ratios are always greater than unity, that is above the horizontal lines in Figure 2.

3.2. Ocean

Figures 3a to 3d compare original and adjusted series of seasonal (January to March, etc.) SST anomalies, relative to the 1961-1990 climatology, for the Northern Hemisphere, Southern Hemisphere, the Niño 3.4 area (5°N-5°S, 120°-170°W), and the Drake Passage (50°-65°S, 40°-80°W). In the latter three areas, coverage has been variable and often sparse, and Figure 3 shows that our adjustments have caused a strong decrease of variance at times of sparse data. Figure 4 shows 10-year running mean standard deviations of monthly anomalies for the same regions to confirm this. Thus there is a much reduced likelihood of obtaining spurious, sampling-related, extreme anomalies. As with the land areas, the grid box SST data are now much more applicable to the analysis of historical changes of the occurrence of true extremes (E.B. Horton et al., The incidence of extremes in worldwide sea surface temperatures and in central England temperatures, submitted to *Climatic Change*, 2000). Figure 5 shows changes in the cumulative frequency distribution, of monthly (Figure 5a) and 6-month (Figure 5b) anomalies for Niño 3.4, based on the 1961-1990 base period, for 1921-1950 and for 1961-1990 itself. Extreme anomalies of either sign have become rarer owing to the removal of the noise. Table 1 gives the associated return periods (the expected elapsed time between specified extremes), which were calculated by fitting a gamma distribution to each sample. Larger changes for monthly anomalies compared to 6-month anomalies are clear, corresponding to greater reductions of standard deviation in monthly than 6-month anomalies. These adjustments, particularly 6-month anomalies, are important to discussions of real changes of ENSO variance between these periods using the original or reconstructed data [e.g., *Kestin et al.*, 1998]. Additionally, Table 1 illustrates the sensitivity of return period calculations to rogue extreme values: the return periods given in parentheses were calculated after the removal of an extreme value of –5.4°C (August 1946) from the 1921-1950 original data sample.

3.3. Combination of the Land and Marine Components of the Surface Temperature Field

The two fields are combined according to the methodology discussed by *Parker et al.* [1994] and more recently by *Jones et al.* [1999b]. Anomaly values are taken from each component field where available. For grid boxes where both land and ocean

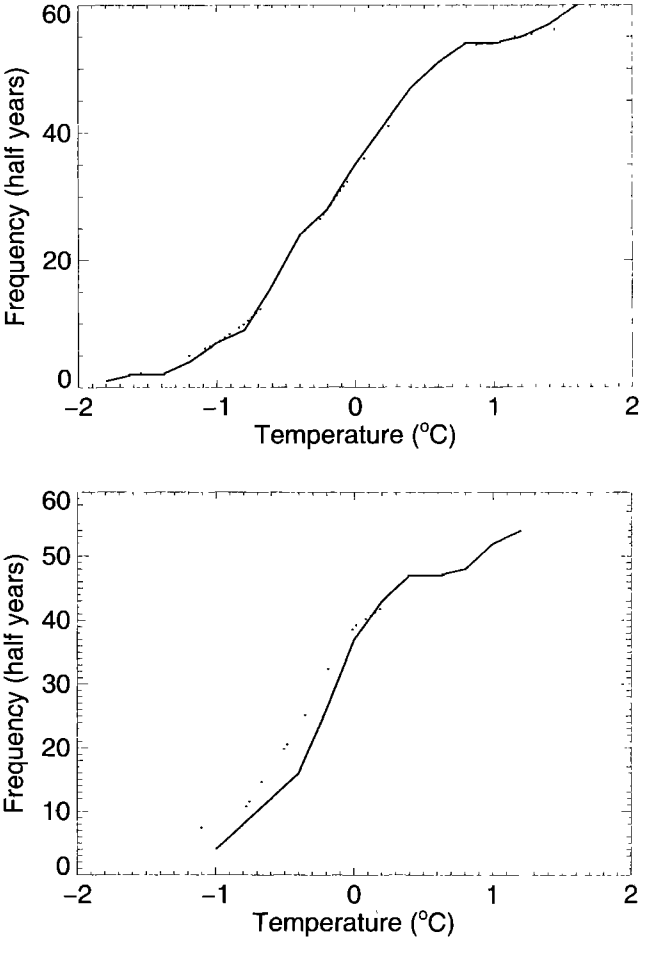

Figure 5b. Cumulative frequency distributions for average 6-monthly temperature anomalies over the Niño3.4 area for adjusted (solid) and unadjusted (dotted) data over (top) 1961-1990 and (bottom) 1921-1950. The anomalies are with respect to 1961-1990 throughout.

Table 1a. Return Periods That Would Be Expected for Various Average Monthly Temperature Anomalies Over 170-120W, 5N-5S (Niño3.4), Calculated From Adjusted and Unadjusted Data and Over Two Different Periods[a]

	Return Period Calculated Over 1961-90, Years		Return Period Calculated Over 1921-1950, Years	
Monthly Anomaly, °C	Original	Adjusted	Original	Adjusted
<-1.5	2	2	1 (1)	14
<-1.75	4	6	1 (3)	69
<-2.0	12	19	2 (9)	-
>1 5	1	1	8 (3)	5
>1 75	2	3	9 (5)	13
>2.0	4	6	- (10)	33

[a]The values in parentheses were calculated after the removal of an erroneous value from the original data. Dashes indicate that the return period calculated was too long compared with the sample size Anomalies are with respect to 1961-1990.

Table 1b. Return Periods That Would Be Expected for Various Average 6-Monthly Temperature Anomalies Over 170-120W, 5N-5S (Niño3.4), Calculated From Adjusted and Unadjusted Data and Over Two Different Periods

	Return Period Calculated Over 1961-1990, Years		Return Period Calculated Over 1921-1950, Years	
6-Monthly Anomaly, °C	Original	Adjusted	Original	Adjusted
<-0.75	2	2	2	4
<-1.0	4	5	4	14
<-1.25	9	10	10	66
<-1.5	21	24	34	-
>0.75	2	3	5	5
>1.0	4	4	11	11
>1.25	6	8	21	25
>1.5	11	14	44	58

data are available, the combined value is weighted, with the weights determined by the fraction of land and ocean in the 5° x 5° box. Because the land component from small oceanic islands is potentially more reliable than surrounding SST values, the land fraction is assumed to be 25% for each box with some, but less than 25%, land. Correspondingly, all ocean fractions are also taken to be 25% for boxes with some, but less than 25% ocean, as some coastal areas have plentiful marine data.

In addition to the merging, some infilling and correction of land grid boxes had been undertaken by *Jones et al.* [1999b] and *Parker et al.* [1994], but it was only explained briefly. Land grid boxes were only corrected or infilled when at least four of the eight surrounding 5° x 5° grid boxes had land-based anomaly data. The mean of the surrounding anomalies was calculated and used to infill the box if it was missing, or if the absolute difference between the existing and the neighbor-based value was greater than 2.25°C. In the present work, however, if a value for the central grid box existed, it was changed to the interpolated value only if the two following conditions were met, in addition to the 2.25°C criterion: (1) only one station was used in calculating the central grid box anomaly and (2) the absolute difference was at least twice the standard deviation of the (existing value minus neighbor-based) monthly time series (based on data for 1921-1990).

3.4. Combined Land and Ocean Time Series

Annual global and hemispheric anomalies (relative to 1961-1990) of combined land surface air temperature and SST since 1871 using the variance-adjusted data are shown in Figure 6. The effects of the adjustments are also shown in the right-hand panels, which present the differences between the series on the left-hand panels and corresponding series using unadjusted data [e.g., *Jones et al.*, 1999b, Figure 2]. The annual changes on these large scales are in the range ±0.06°C in the late 19th century, declining to ±0.03°C by the end of the 20th century. These changes are consistent with *Jones et al.* [1997] as the effect of changing station numbers on variance is one of the components of the standard error of the estimates due to sampling. The other components are errors caused by areas missing from the analysis and uncertainties due to biases or in bias corrections.

4. Conclusions

We have developed methods to adjust grid box time series of land surface air temperature and SST to account for changing numbers of contributing data through time. After adjusting the grid box variances to consistent levels, results concerning variances or extremes derived from the data need no longer be

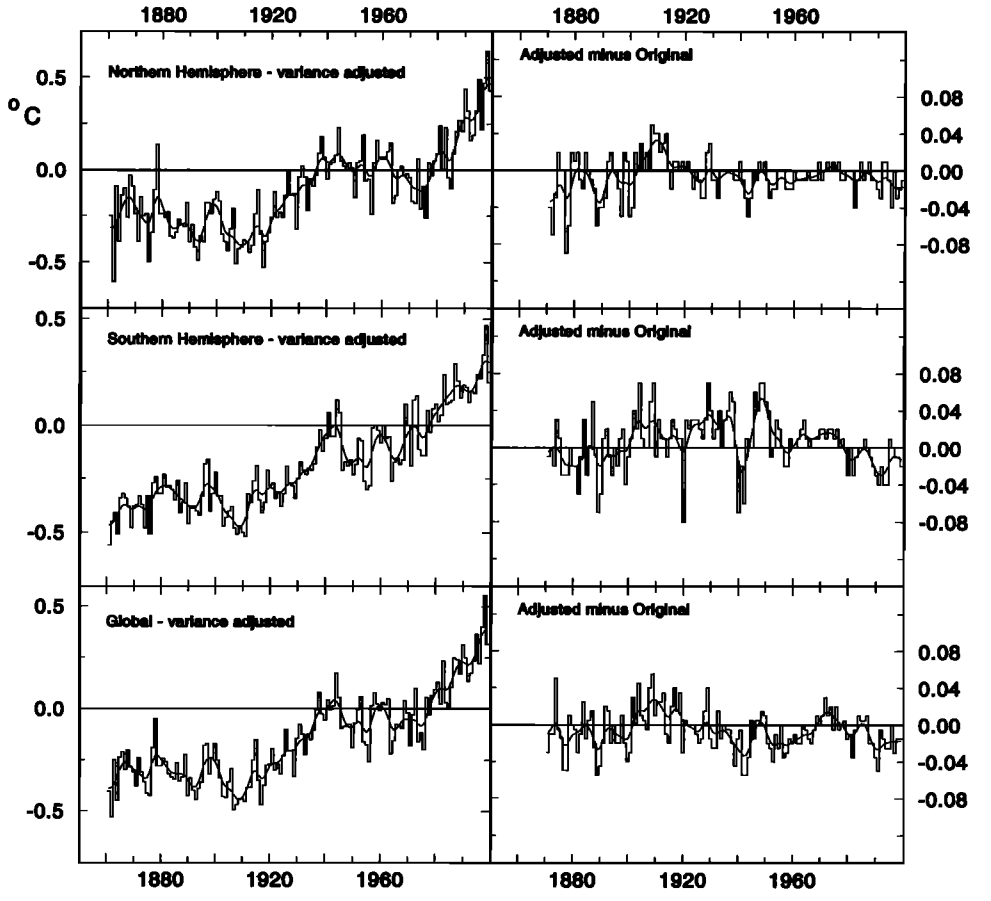

Figure 6. Annual hemispheric and global temperature anomalies (°C), relative to the 1961-1990 average, of combined land surface air temperature and SST since 1870 using variance-adjusted data. The plot includes data for 1861-1870, for completeness, but the first 10 years are not variance adjusted. (right) Differences (°C) between the series on the left and corresponding series using unadjusted data [e.g., *Jones et al.*, 1999b, Figure 2]. All series are also plotted smoothed with a 10-year Gaussian filter. Note the differences in the vertical scales between the left- and right-hand side of the plot.

qualified by such restrictive caveats relating to changing data density where data exist. These adjustments do not account for uncertainties where no data exist. The most important application of the adjustments is to estimates of how unusual anomalies are in given regions or in regions covered by extremes. The adjustments are mostly relatively small over land, but they tend to be larger over data-sparse ocean areas. The adjusted data set will enable more reliable estimates to be made of covariance/correlation matrices necessary for PCA/EOF techniques. An early version of the adjusted oceanic data that did not include COADS data has been used to provide improved local detail in the HadISST1 data set (Rayner et al., manuscript in preparation, 2000), used as a lower boundary forcing in simulations of the global climate since the late 19th century. The land surface air temperature data set is known as CRUTEM1 and the sea surface temperature data set uses the new naming convention and is called the Hadley Centre Sea Surface Temperature data set version 1 (HadSST1). The combined variance-corrected version is HadCRUTv, with the original (nonvariance adjusted) version being HadCRUT. All four data sets (CRUTEM1, HadSST1, HadCRUT, and HadCRUTv) are available on the Climatic Research Unit web site (http://www.cru.uea.ac.uk).

Acknowledgments. This work was supported by the U.S. Department of Energy (grant DE-FG02-98ER62601), the U.K Department of the Environment, Transport and the Regions (contract PECD/7/12/37), and by the U.K Public Meteorological Service Research and Development Programme, contract MSG 2/99

References

Bottomley, M., C.K. Folland, J Hsiung, R.E. Newell, and D.E. Parker, *Global Ocean Surface Temperature Atlas "GOSTA"*, 20 pp.+iv, 313 plates, Her Majesty's Stn. Off., Norwich, England, 1990.

Briffa, K.R., and P.D. Jones, Basic chronology statistics, in *Methods of Dendrochronology: Applications in the Environmental Sciences*, edited by E.R Cook and L A. Kairiukstis, pp.137-152, Kluwer Acad , Norwell, Mass., 1990.

Briffa, K.R., P.D. Jones, F.H. Schweingruber, and T J Osborn, Influence of volcanic eruptions on Northern Hemisphere summer temperature, *Nature, 393*, 450-455, 1998.

Hansen, J.E., and S. Lebedeff, Global trends of measured surface air temperature, *J. Geophys. Res., 92*, 13,345-13,372, 1987

Hansen, J , R. Ruedy, J. Glascoe, and M. Sato, GISS analysis of surface temperature change, *J. Geophys Res., 104*, 30,997-31,022, 1999.

Jones, P.D., Hemispheric surface air temperature variations: A reanalysis and an update to 1993, *J. Clim., 7*, 1794-1802, 1994.

Jones, P.D., S.C B. Raper, R.S. Bradley, H.F Diaz, P.M. Kelly, and T.M L Wigley, Northern Hemisphere surface air temperature variations: 1851-1984, *J. Clim. Appl Meteorol , 25*, 161-179, 1986.

Jones, P.D , T J. Osborn, and K.R Briffa, Estimating sampling errors in large-scale temperature averages, *J. Clim., 10*, 2548-2568, 1997

Jones, P.D., E.B Horton, C.K. Folland, M. Hulme, D.E. Parker, and T.A. Basnett, The use of indices to identify changes in climatic extremes, *Clim. Change*, *42*, 131-149, 1999a.

Jones, P.D , M. New, D E. Parker, S. Martin, and I G Rigor, Surface air temperature and its changes over the past 150 years, *Rev. Geophys.*, *37*, 173-199, 1999b.

Kagan, R.L., *Averaging of Meteorological Fields*, edited by L S Gandin and T.M. Smith, 279 pp , Kluwer Acad., Norwell, Mass., 1997.

Kaplan, A., M.A. Cane, Y. Kushnir, A C. Clement, M.B. Blumenthal, and B. Rajagopalan, Analyses of global sea surface temperature 1856-1991, *J. Geophys. Res.*, *103*, 18,567-18,589, 1998

Kent, E.C., P.G. Challenor, and P.K Taylor, A statistical determination of the random observational errors present in Voluntary Observing Ships' meteorological reports, *J Atmos Oceanic Technol.*, *16*, 905-914, 1999

Kestin, T.S., D.J. Karoly, J -I. Jano, and N A Rayner, Time-frequency variability of ENSO and stochastic simulations, *J Clim.*, *11*, 2258-2272, 1998.

Osborn, T.J., and M. Hulme, Development of a relationship between station and grid-box rainday frequency for climate model evaluation, *J. Clim.*, *10*, 1885-1908, 1997

Osborn, T J., K R. Briffa, and P.D. Jones, Adjusting variance for sample size in tree-ring chronologies and other regional-mean timeseries, *Dendrochronologia*, *15*, 89-99, 1997

Parker, D.E., T P. Legg, and C.K Folland, A new daily central England temperature series, 1772-1991, *Int. J. Climatol* , *12*, 317-342, 1992.

Parker, D E., P.D. Jones, A. Bevan, and C K. Folland, Interdecadal changes of surface temperature since the 19th century, *J Geophys. Res.*, *99*, 14,373-14,399, 1994.

Parker, D.E , C.K. Folland, and M Jackson, Marine surface temperature: Observed variations and data requirements, *Clim Change*, *31*, 559-600, 1995.

Peterson, T.C., T.R. Karl, P.F. Jamason, R. Knight, and D.R. Easterling, The first difference method: Maximizing station density for the calculation of long-term global temperature change, *J. Geophys. Res.*, *103*, 25,967-25,974, 1998.

Rayner, N.A., E.B. Horton, D.E. Parker, C.K. Folland, and R.B. Hackett, Version 2.2 of the global sea-ice and sea surface temperature data set, 1903-1994, *Climate Res. Tech. Note*, *74*, Hadley Cent., U.K. Meteorological Office, Bracknell, U K., 1996

Wigley, T.M L., K.R. Briffa, and P.D. Jones, On the average value of correlated time series with applications in dendroclimatology and hydrometeorology, *J. Clim. Appl. Meteorol.*, *23*, 201-213, 1984.

Woodruff, S D., R.J. Slutz, R.L. Jenne, and P.M. Steurer, A comprehensive ocean-atmosphere data set, *Bull. Am. Meteorol Soc.*, *68*, 1239-1250, 1987.

Woodruff, S D., H.F. Diaz, J D. Elms, and S.J. Worley, COADS release 2 data and metadata enhancements for improvements of marine surface flux fields, *Phys. Chem. Earth*, *23*, 517-526, 1998.

Yevjevich, V , *Probability and Statistics in Hydrology*, 302 pp., Water Resour. Publ , Highlands Ranch, Colo., 1972.

L V Alexander, C.K Folland, E.B. Horton, D E Parker, and N.A. Rayner, Hadley Centre for Climate Prediction and Research, The Met. Office, Bracknell, RG12 2SY, Berkshire, U K.

K.R. Briffa, P.D. Jones, and T.J. Osborn, Climatic Research Unit, University of East Anglia, Norwich, NR4 7TJ, U K (p jones@uea ac.uk)

(Received April 29, 2000; revised August 17, 2000; accepted August 24, 2000.)